Supporting information

A core/satellite multifunctional nanotheranostic for *in vivo* imaging and tumor eradication by radiation/photothermal synergistic therapy

Qingfeng Xiao,[†] Xiangpeng Zheng,[‡] Wenbo Bu,*[,†] Weiqiang Ge,[‡] Shengjian Zhang,[§] Feng Chen,[†] Huaiyong Xing,[†] Qingguo Ren,[‡] Wenpei Fan,[†] Kuaile Zhao,[§] Yanqing Hua,[‡] and Jianlin Shi*[,†]

[†]State Key Laboratory of High performance Ceramics and Superfine Microstructures, Shanghai Institute of Ceramics, Chinese Academy of Sciences, Shanghai, 200050 (P.R. China)

[‡]Department of radiation oncology, Shanghai Huadong Hospital, Fudan University, Shanghai, 200040, (P.R. China)

[§]Department of radiology, Shanghai Cancer Hospital, Fudan University, Shanghai, 200032, (P.R. China)

Section 1: Experimental

Chemicals and reagents. Sodium citrate, Cupric chloride ($CuCl_2 \cdot 2H_2O$), Cyclohexane, Sodium sulfide ($Na_2S \cdot 9H_2O$), Ammonium hydroxide ($NH_3 \cdot H_2O$), was purchased from Sinopharm Chemical Reagent Co., China. Rare-earth chlorides (99.9%), Oleic acid (OA), 1-Octadecene（90%）, Igepal CO-520 (NP-5) and 3-Aminopropyl-triethoxysilane (APTES, 99%) were purchased from Sigma-Aldrich. O-[2-(3-Mercaptopropionylamino)ethyl]-O′ -methylpolyethyleneglycol (PEG5000-SH) was obtained from Jenkem Technology Co., China. NaOH, NH_4F, CH_3OH, CH_3CH_2OH and TEOS were obtained from Shanghai Lingfeng Chemical Reagent Co., LTD. All reagents were of analytical grade and used without any purification. Deionized water was used throughout the experiments.

Preparation of $NaYb(78\%)F_4$: Gd^{3+} (20%)/ Er^{3+} (2%) nanocrystal. Firstly, these Yb-based UCNPs were synthesized by thermal decomposition using our previously reported procedures with minor modifications.[1] $YbCl_3 \cdot 6H_2O$ (604.4 mg, 1.56 mmol), $ErCl_3 \cdot 6H_2O$ (15.3 mg, 0.04 mmol) and $GdCl_3 \cdot 6H_2O$ (148.7 mg, 0.4 mmol) in deionized water were added to a 100 mL flask containing 15 mL oleic acid and 30 mL 1-octadecene. The solution was stirred at room temperature for 1 h. Then the mixture maintained at 156 °C for about 1 h until a homogeneous transparent yellow solution was obtained. The system was then cooled down to room temperature with the flowing of argon before adding 10 mL methanol solution of NH_4F (296.3 mg, 8 mmol) and NaOH (200 mg, 5 mmol). After methanol evaporated, the solution was heated to 280-290 °C for 1.5 hours and then cooled down to room temperature. The resulting nanoparticles were precipitated by the addition of 20 mL ethanol and collected by centrifugation. The product was redispersed with 10 mL cyclohexane and precipitated by adding 20 mL ethanol, then collected by centrifugation. After four times' washing, the final product was finally dispersed in 20 mL cyclohexane.

Synthesis of positively charged UCNP@SiO_2–NH_2 nanoparticles with water-in-oil reverse microemulsion strategy. The synthesis of UCNP@SiO_2–NH_2 was carried out using procedures reported by our group.[2] As-prepared Yb-based UCNP-cyclohexane solution (1.5 ml) was added into the mixture of Igepal CO-520 (NP-5, 1 mL) and cyclohexane (20 mL). After stirring for 3 h, $NH_3 \cdot H_2O$ (150 μL, 30%) was added and the mixture was stirred for another 2 hours. A Syringe Pump was used to control the adding rate, and the solution (1 mL) composed of TEOS (0.2 mL) and cyclohexane (0.8 mL) was introduced into the system within 1 h. The system was hermetically stirred for 24 h. To graft amino-groups, 50 μL APTES was added into the system and stirred for another 5 h. Then methanol was added to precipitate the product before collecting nanoparticle by centrifugation. The as-prepared nanoparticle was redispersed in ethanol under ultrasonic treatment, precipitated with excess hexane, and collected by centrifugation. This procedure was repeated for three times to remove excess NP-5. The as-obtained nanoparticles were finally dispersed in 20 mL deionized water.

Preparation of CSNTs with electrostatic adsorption technique. Firstly, negatively charged citrate-stablized CuS nanoparticles were synthesized using previously reported procedures.[3, 4] $Na_2S \cdot 9H_2O$ solution (2 mL, 0.05 M) was added into 100 mL of the aqueous solution of $CuCl_2 \cdot 2H_2O$ (17 mg, 0.1 mmol) and sodium citrate (0.02 g, 0.068 mmol) with stirring at the room temperature. After 5 min, the dark-brown mixture was transferred to the water bath at the temperature of 80 ℃ and stirred for 10 min until the color of solution turn into

dark-green. Then, the mixture was immediately placed in the ice-cold water. The as-prepared CuS solution (60 mL) was mixed with UCNP@SiO_2-NH_2 (10 mL) with stirring for 40 min. The products were collected by centrifugation and dispersed in the 20 mL deionized water. Then 60 mg PEG5000-SH was added with ultrasonic treatment for 10 min. The mixture was stirred for another 12 h at the room temperature. The PEG modified nanotheranostics were then centrifuged and washed with water for three times. CSNTs were finally obtained.

Assessment of CSNTs as radiosensitizers. The assessment of radiosensitizing effect of CSNTs was conducted on the polymer gels whose T_2-weighted signal changed with radiation. The mechanism is as follow: MRI-mediated polymer gels dosimetry is established mainly based on the radiation-induced free radical polymerization and their subsequent relaxation time measurements using magnetic resonance. It is known that polymerization can be initiated by radiation via free radical production during water radiolysis. The polymerization level is highly dependent on the initial quantity of free radicals generated by the incident radiation dose. In the polymerized regions, a proportion of water molecules will alter their state of binding to, and exchange protons with, the polymer network. This kind of variation can just be directly detected by magnetic resonance (MR) transverse relaxation time measurements. Therefore, MR imaging is usually reported to visualize the radiation dose on these polymer gels.[5-9] The higher radiation dose we use, the stronger MR signal the gels display. In this study, the radiosensitive MAGIC (Methacrylic and Ascorbic acid in Gelatin Initiated by Copper) gel was prepared as previously reported with minor modification.[9] Typically, 8 g of gelatin was mixed with 70 mL of water and stirred for at 50 °C for 30 min before adding 200 mg of hydroquinone in 4.8 mL of water. Then the solution was cooled down to 37 °C, followed by adding ascorbic acid (35.2 mg in 5 mL of water), $CuSO_4$•$5H_2O$ (2 mg in 3 mL of water) and 9 g of methacrylic acid and stirring for 1 h. After that, 55 mg of CSNTs were introduced and stirred for another 1 h. The MAGIC gels were transferred in a refrigerator at 4 °C overnight. After irradiated under radiotherapy instrument at the dose of 6 Gy, the Gels were scanned using a clinical MR scanner (TR 8 s, TE 40 ms).

***In vivo* investigation.** Healthy Balb/c female mice (~20 g) were obtained and raised at Laboratory animal center, shanghai medical college of Fudan University. Animal procedures were in agreement with the guidelines of the Regional Ethics Committee for Animal Experiments. All anesthetization was performed by intraperitoneal injection of 10% chloral hydrate (50 μL). Hair on the flanks of the mice was removed before they received any further treatments.

Charaterization of CSNTs. The morphology and Energy-dispersive X-ray analysis (EDX) of the nanotheranostic were performed on a JEOL 200CX microscope operated at 200 kV with nickel grid. Dynamic light scattering (DLS) was performed on Nano-Zetesizer (Malvern Instruments Ltd). Fourier transform infrared spectroscopy (FT-IR) spectra were recorded on a Nicolet 7000-C spectrometer by using pressed KBr tablets. Upconversion luminescence emission spectra were collected on Fluorolog-3 Spectrofluorometer (Jobin Yvon, France), with the excitation of a 450 W xenon lamp and an external 0 ~ 1 W adjustable 980 nm semiconductor laser (Beijing Hi-tech Optoelectronic Co., China). The radiotherapy of tumor-bearing mice was accomplished on Siemens Primus clinical accelerator (6 MeV) with 6 Gy radiations in a 1.5 × 3 cm field with SSD 100 cm. The MR imaging experiments were performed on a 3.0-T clinical MRI instrument (GE Signa 3.0-T), and the pulse sequence used was a T_1-weighted FSE-XL/90 sequence with the following parameters: TR/TE = 1000, 2000, 3000, 4000/7.9 ms: field of view [FOV]: 18 cm; matrix: 128 × 128; number of excitations (NEX): 2; slice thickness = 2 mm; space = 0.5 mm; FOV: 18 cm; coil: QUADKNEE. The CT tests were performed on GE discovery CT750 HD, GE Healthcare, WI with

5 mm slice thickness and 5 mm interval at 120 kVp and 100 mAs with the following parameters: beam collimation, 64 × 0.625 mm; table speed, 27 mm per rotation; beam pitch, 1.25; gantry rotation time, 1.0 s.

Reference

(1) Chen, F.; Bu, W.; Zhang, S.; Liu, X.; Liu, J.; Xing, H.; Xiao, Q.; Zhou, L.; Peng, W.; Wang, L.; Shi, J. Adv. Funct. Mater. **2011**, *21*, 4285.

(2) Xing, H.; Bu, W.; Zhang, S.; Zheng, X.; Li, M.; Chen, F.; He, Q.; Zhou, L.; Peng, W.; Hua, Y.; Shi, J. Biomaterials **2012**, *33*, 1079.

(3) Zhou, M.; Zhang, R.; Huang, M.; Lu, W.; Song, S.; Melancon, M. P.; Tian, M.; Liang, D.; Li, C. J. Am. Chem. Soc. **2010**, *132*, 15351.

(4) Li, Y.; Lu, W.; Huang, Q.; Li, C.; Chen, W. Nanomedicine **2010**, *5*, 1161.

(5) Doran, S. J. Appl. Radiat. Isot. **2009**, *67*, 393.

(6) McJury, M.; Oldham, M.; Cosgrove, V. P.; Murphy, P. S.; Doran, S.; Leach, M. O.; Webb, S. Br. J. Radiol. **2000**, *73*, 919.

(7)Baldock, C.; De Deene, Y.; Doran, S.; Ibbott, G.; Jirasek, A.; Lepage, M.; McAuley, K. B.; Oldham, M.; Schreiner, L. J. Phys. Med. Biol. **2010**, *55*, R1.

(8) MacDougall, N.; Pitchford, W. G.; Smith, M. A. Phys. Med. Biol. **2002**, *47*, R107.

(9) Fong, P. M.; Keil, D. C.; Does, M. D.; Gore, J. C. Phys. Med. Biol. **2001**, *46*, 3105.

Section 2: Supplementary tables and figures

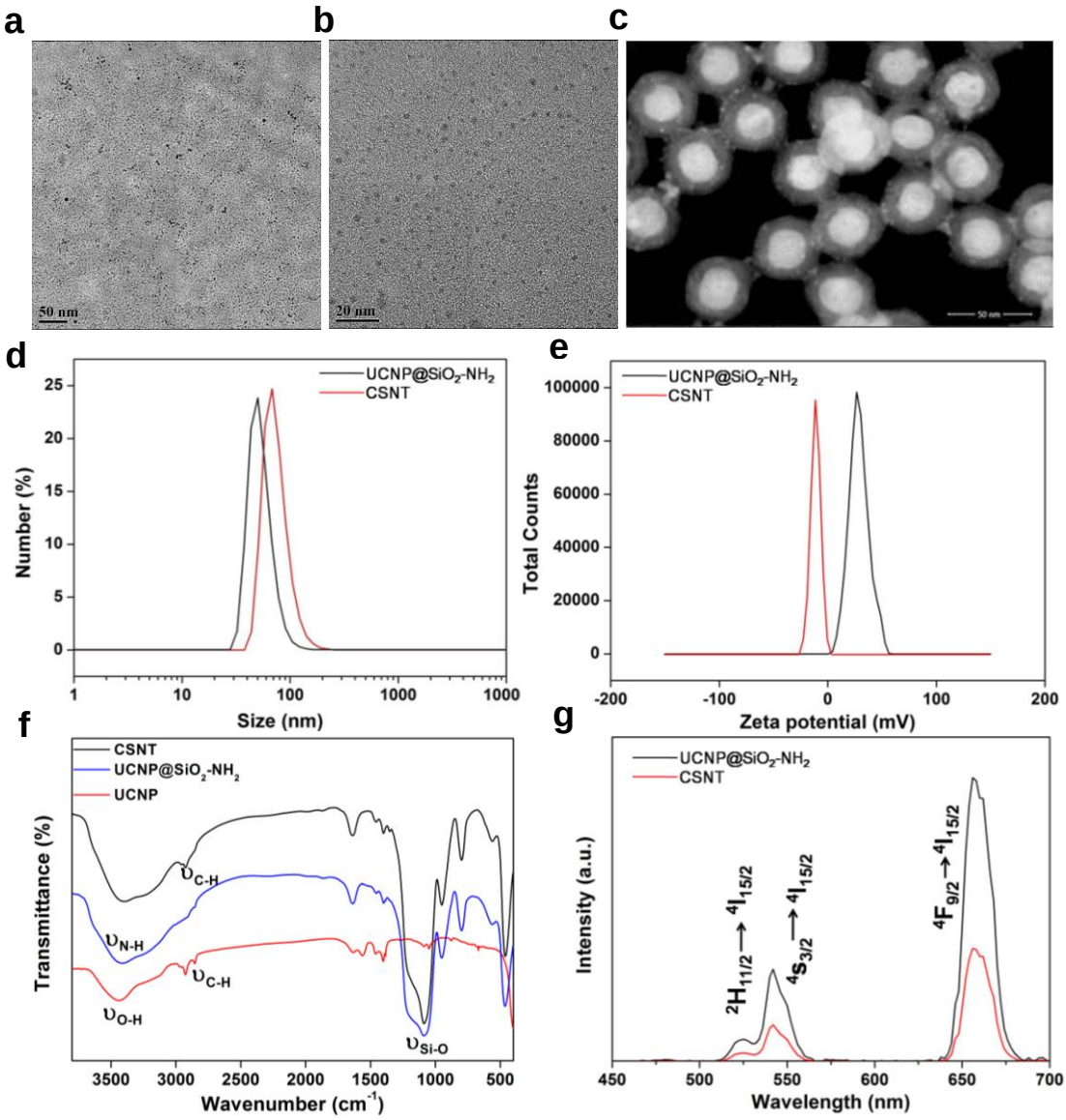

Figure S1. Characterization of the CSNTs. (a, b) Transmission electron microscopy images of CuS nanoparticles at different magnifications. (c) Dark-field STEM image of CSNT. (d, e) Hydrodynamic diameter distributions and Zeta potentials of UCNP@SiO_2-NH_2 and CSNT. Apparently, the absorption of the citrate-stablized CuS nanoparticles on the surface of UCNP@SiO_2-NH_2 has caused the zeta potential change from the positive to the negative. (f) FT-IR spectra of UCNP, UCNP@SiO_2-NH_2 and CSNT. For hydrophobic oleate capped UCNP, the transmission bands located at 2925 and 2852 cm^{-1} could be assigned to stretching vibrations of methylene groups (–CH_2) in the long alkyl chain of OA. The 3442 cm^{-1} band is for the stretching vibration of the O–H (COOH). After coating SiO2 shell and the modification of APTES (aminopropyltriethoxysilane), original peaks at 2925 and 2852 cm^{-1} become greatly weakened with new bands showing up at 1090 cm^{-1} assigned to the asymmetric vibration modes and 463 cm^{-1} for the deformation vibration of the Si–O–Si bond; the broad peak at 3415 cm^{-1} should be attributed to the

stretching and bending vibrations and of N–H. The grafting of PEG5000–SH (o-[2-(3-Mercaptopropionylamino) ethyl] -o′ -methylpolyethylene glycol) leads to the reappearance of stretching vibration bands of the CH_2 and CH_3 at 2925 and 2952 cm^{-1}. The stretching vibration of C–O–C was overlapped with the wide Si–O–Si asymmetric stretching vibration band at 1090 cm^{-1}. These changes of characteristic peaks demonstrate the successful surface modification. (g) Room temperature UCL spectrum of CSNT aqueous solution under the excitation of 980 nm NIR laser. Remarkably, the UCL emission intensity of CSNTs is reduced by about 60% due to lots of ultrasmall CuS satellites. However, fortunately, it will not pose a great obstacle to CSNTs' role in cellular localization because of high sensitivity of fluorescence imaging.

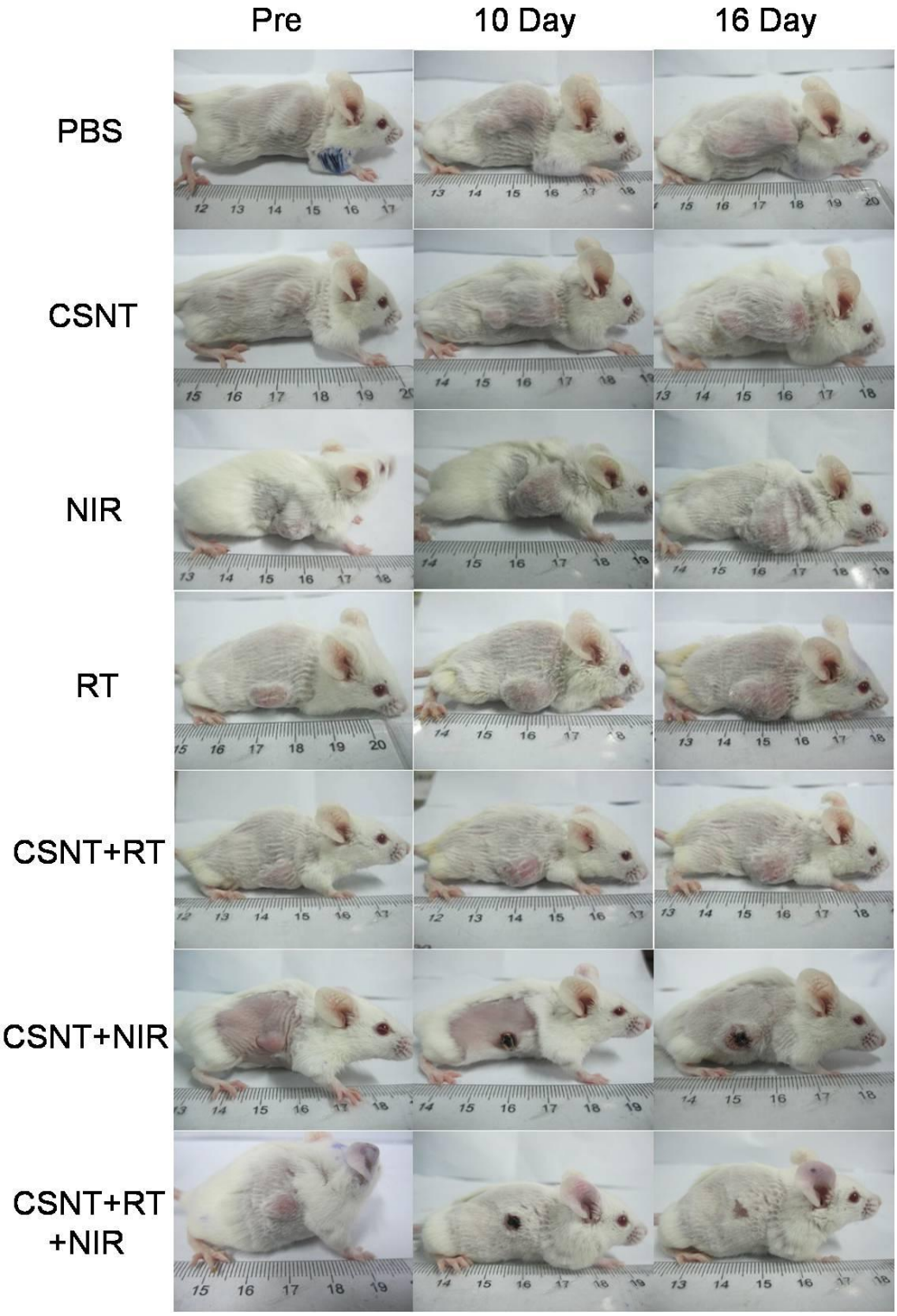

Figure S2. Representative gross photographs of the mice before and after various treatments at varied time points of 10 and 16 days.

Table S1. The relative tumor volumes ($R = V/V_0$) and tumor growth inhibition (TGI) in each group at the 16th day after various treatments. TGI (%) =100 × (R_1 - R_n) / R_1, where R_1 is the relative tumor volume of the group 1 and R_n is the relative tumor volume of the nth group. (1) PBS alone; (2) CSNT alone; (3) laser alone; (4) RT alone; (5) CSNT + RT; (6) CSNT + laser; (7) CSNT + RT + laser. The above treatments are based on intratumoral injection.

	Group 1	Group 2	Group 3	Group 4	Group 5	Group 6	Group 7
V/V_0	6.2±0.47	5.9±0.43	6±0.4	3.8±0.5	2.3±0.51	1.3±0.42	0
TGI	—	—	—	38.7%	62.9%	79%	100%

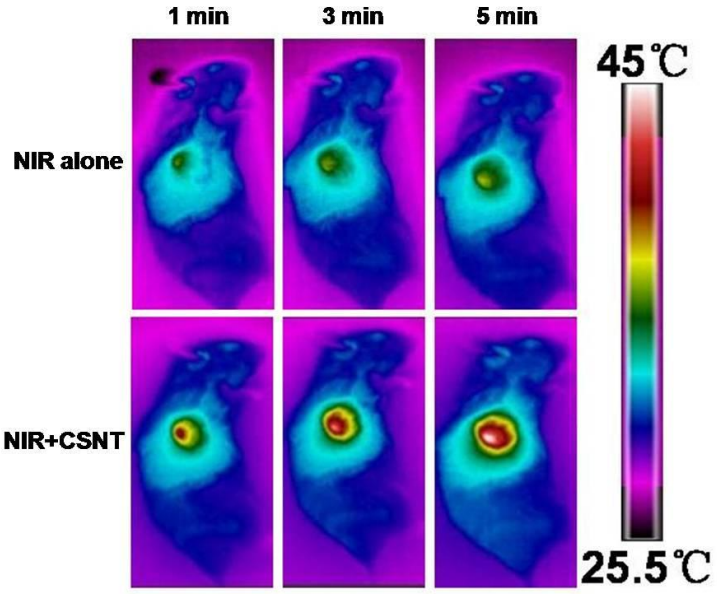

Figure S3. Infrared thermal mapping experiment in a tumor-bearing mouse carried out after intratumoral injection of CSNTs （1.2 mg/mL, 150 μL） with the excitation of 980 nm at the power density of 1.5 W/cm² in 5 min. During the irradiation, the tumor surface temperature rapidly increased (NIR+CSNT), while in the comparative experiments, tumor temperature of mice without CSNT injection under the same laser irradiation displays a very limited variation (NIR alone). These results indicate the feasible photothermal conversion by CSNT.

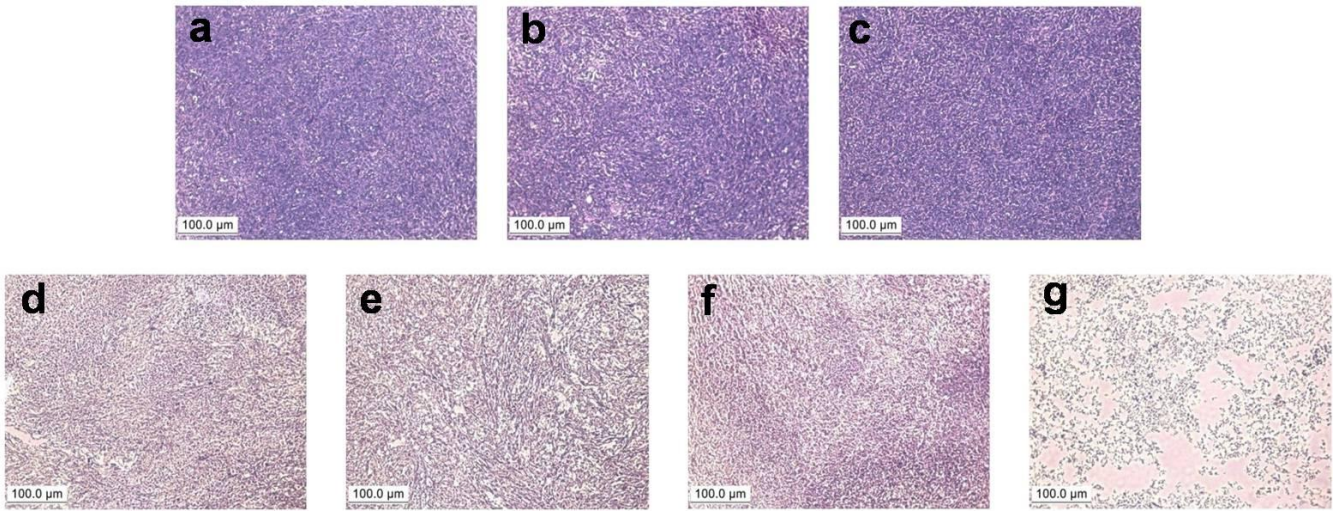

Figure S4. Histological assessments of tumor tissues collected from different groups of mice receiving various treatments: a) PBS; (b) CSNT alone; (c) NIR alone; (d) RT alone; (e) CSNT+RT; (f) CSNT+NIR; (g) CSNT+RT+NIR

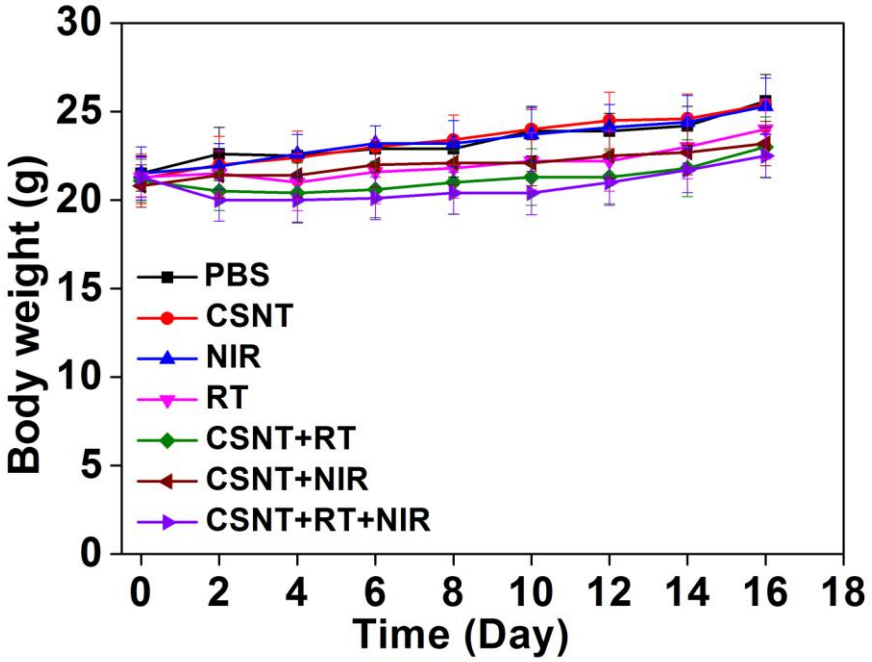

Figure S5. Body weight changes after various treatments exhibiting no significant influence of CSNT on the health status of mice.

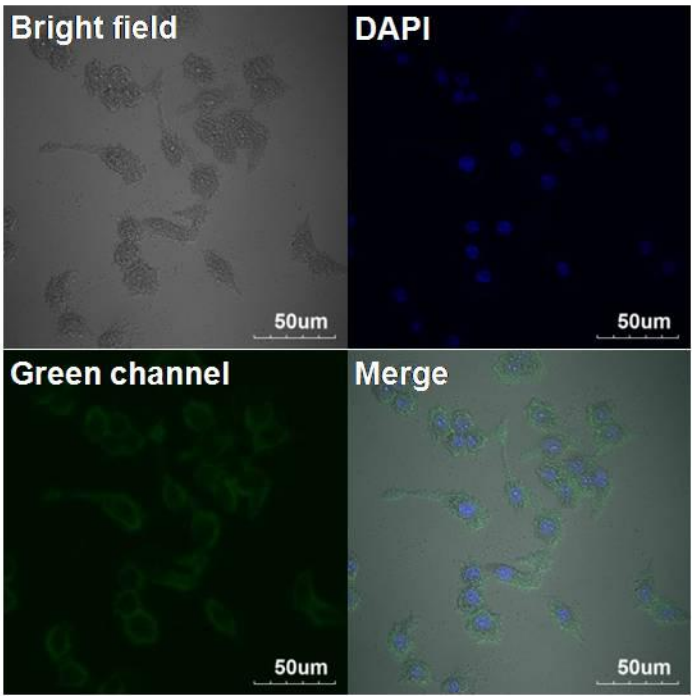

Figure S6. Confocal fluorescence imaging of Hela cells incubated with CSNTs for 4 h. The nuclei were stained blue with 4′-6-diamidino-2-phenylindole (DAPI).

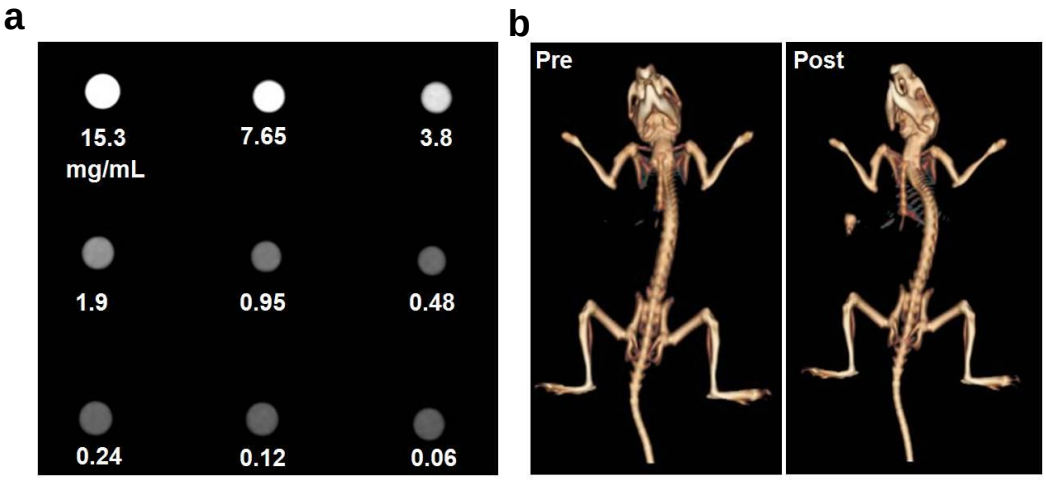

Figure S7. The feasibility of CSNTs as CT contrast agents. (a) CT images of CSNTs solution at varied concentrations (the values stand for the total concentration of rear earth elements (Yb, Gd and Er) in corresponding sample which played a dominant role in CT imaging). (b) CT volume-rendered images of tumor at before and after intravenous injection of CSNTs (the corresponding total concentration of rare earth elements: 8 mg/mL, 150 μL).

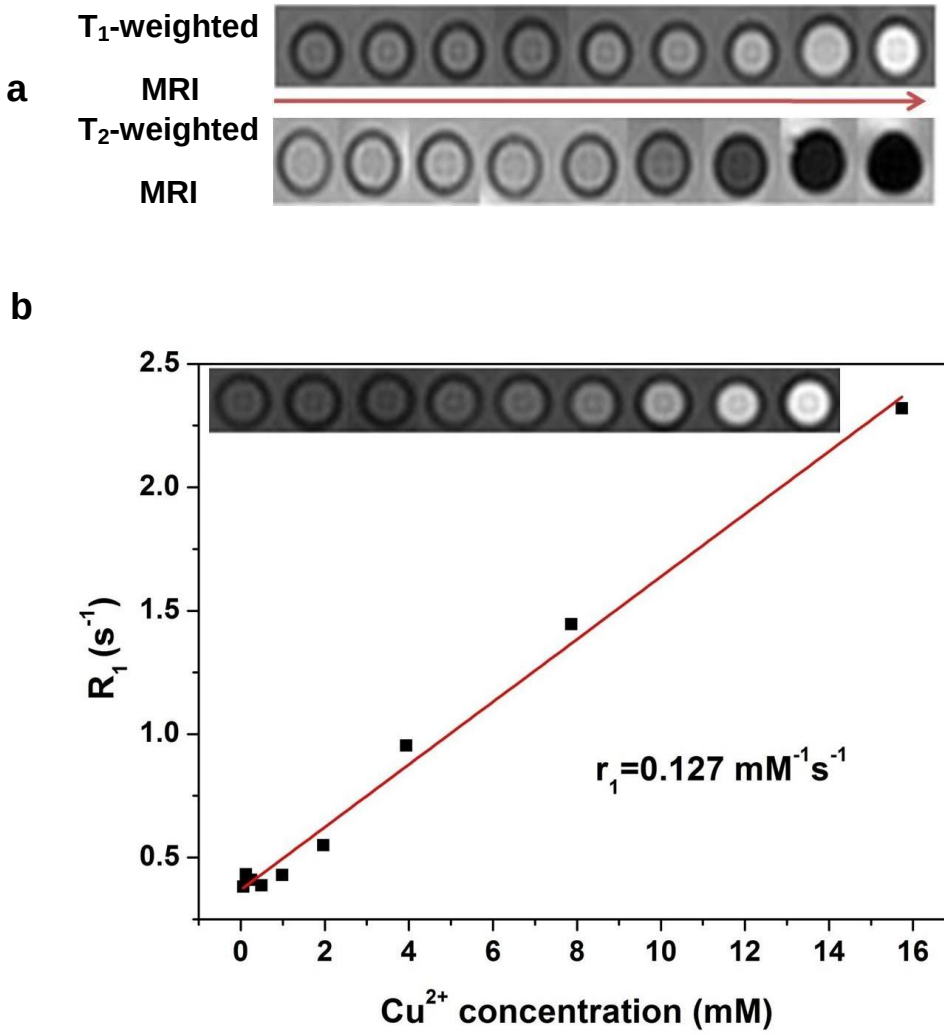

Figure S8. MR images of CSNTs and CuS nanoparticles. (a) T_1- and T_2-weighted MR images of CSNTs at different concentrations from 0 mg/mL to 2.52 mg/mL (water) along the direction of the arrow. (b) T_1-weighted MR images (inset) and relaxation rate R_1 ($1/T_1$) versus Cu^{2+}-concentration of CuS aqueous solution. The concentration-dependent enhancement of brightness in CuS solution (inset) and the longitudinal relaxivity (0.127 $mM^{-1}s^{-1}$) demonstrate that CuS could make a certain contribution to the T_1-weighted MR imaging.

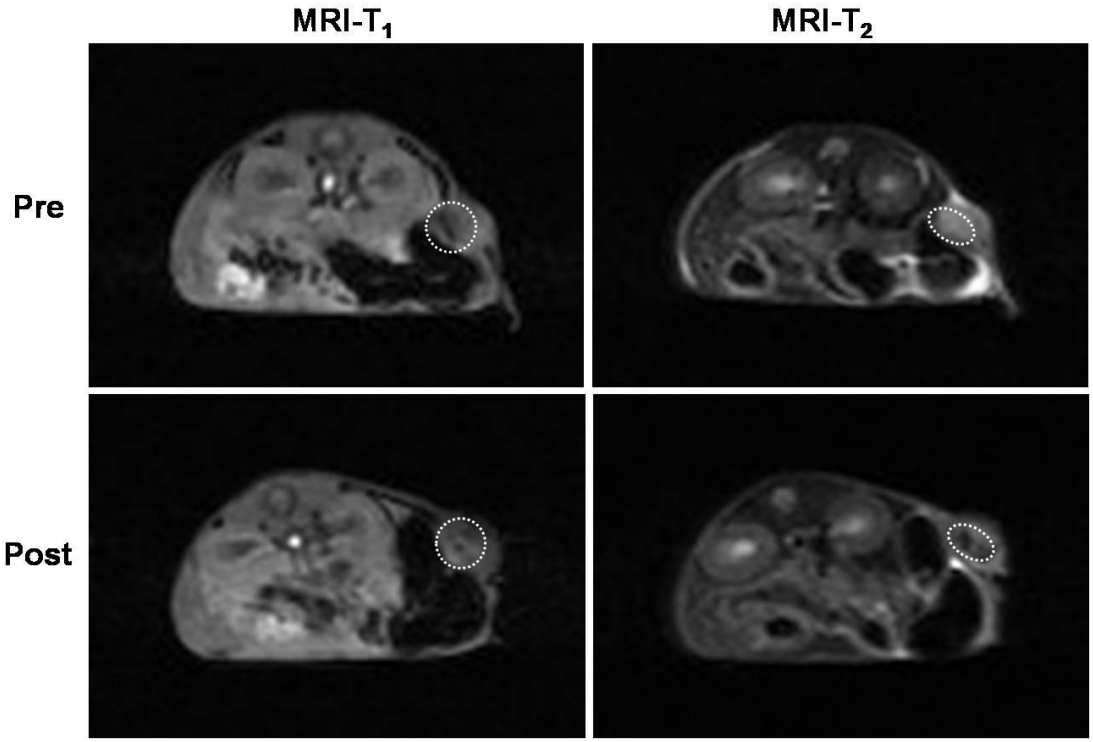

Figure S9. *In vivo* MR imaging of CSNTs. T_1- and T_2- weighted MR images of a tumor site before and after intra-tumoral injection of CSNTs (1.97 mg/mL, 150 μL).

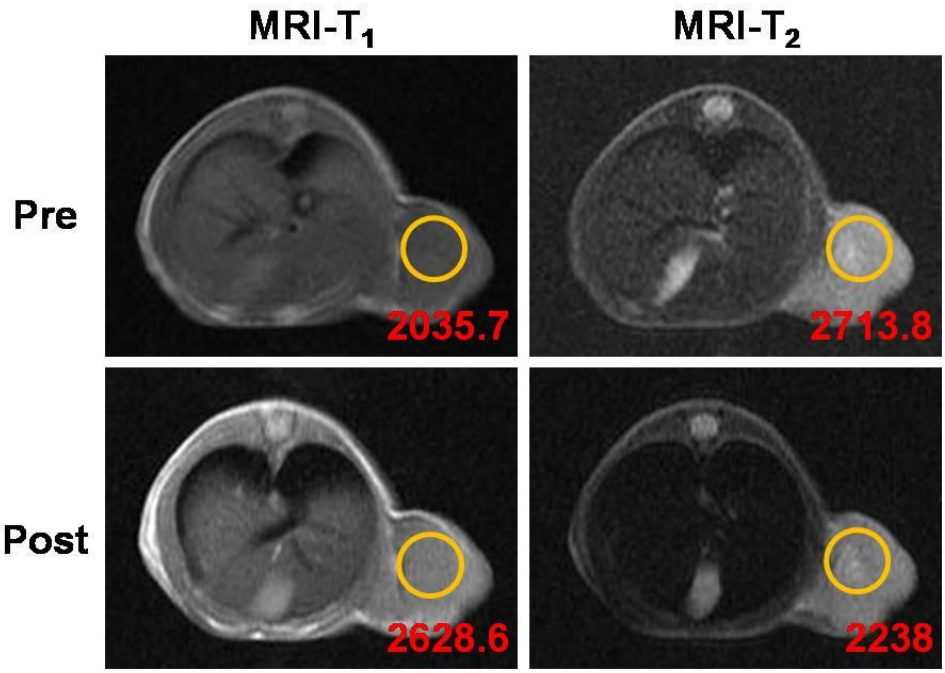

Figure S10. *In vivo* MR imaging of CSNTs. T_1- and T_2- weighted MR images of a tumor site before and 1.5 h after intravenous injection of CSNTs (13.2 mg/mL, 150 μL). The tumor sites are marked with the circles.

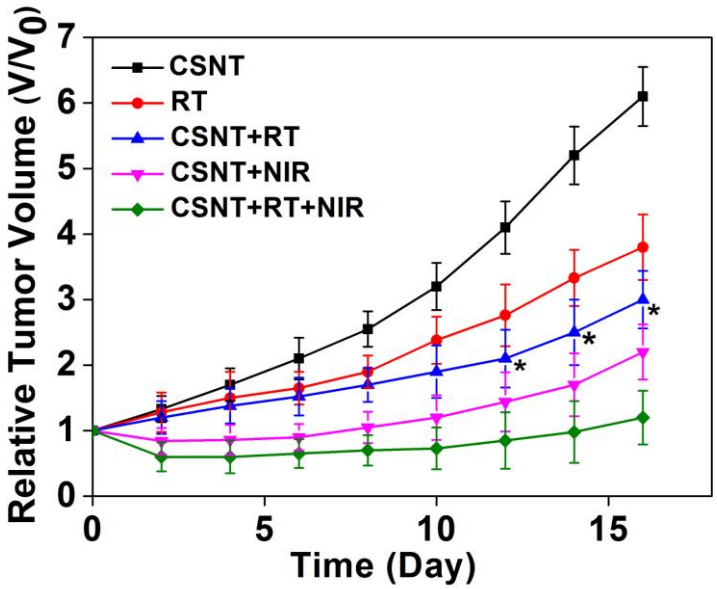

Figure S11. Time-dependent tumor growth curves of different groups of mice receiving various treatments. Mice were intravenously injected with CSNTs. Significant difference between RT alone and CSNT+RT groups at the 16th day demonstrates CSNTs' important role in the increased RT efficacy (*P=0.0147). Statistical analysis was performed using the Student's two-tailed t test (*P<0.05).

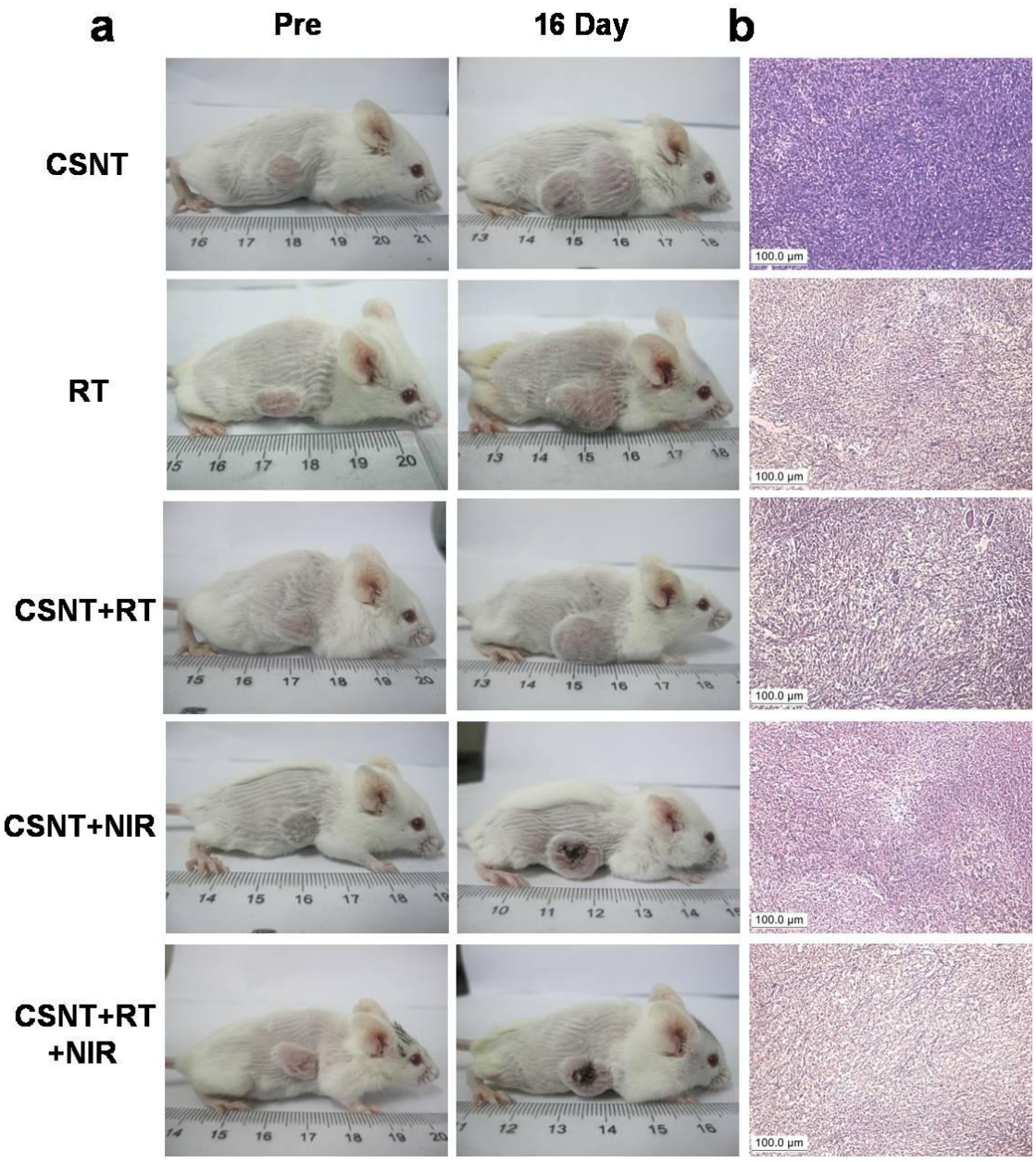

Figure S12. (a) Representative gross photographs of the mice before and after various treatments. Mice were intravenously injected with CSNTs. (b) Histology investigation of tumors subjected to various treatments. Remarkably, the most significant tumor damage appears in the CSNT+RT+NIR group.

Table S2. The relative tumor volumes ($R = V/V_0$) and tumor growth inhibition (TGI) of mice intravenously injected with CSNTs at the 16th day after various treatments. (1) CSNT alone; (2) RT alone; (3) CSNT + RT; (4) CSNT + NIR; (5) CSNT + RT + NIR.

	group 1	group 2	group 3	group 4	group 5
V/Vo	6.1±0.42	3.8±0.5	3.0±0.44	2.2±0.42	1.2±0.41
TGI	—	37.7%	50.8%	63.9%	80.3%